Dating of the GV7 East Antarctic ice core by high resolution chemical records and focus on the accumulation rate variability in the last millennium

Raffaello Nardin[1], Mirko Severi[1,2*], Alessandra Amore[1], Silvia Becagli[1,2], Francois Burgay[3,4], Laura Caiazzo[5], Virginia Ciardini[6], Giuliano Dreossi[2,3], Massimo Frezzotti[7], Sang-Bum Hong[8], Ishaq Khan[3], Bianca Maria Narcisi[6], Marco Proposito[6], Claudio Scarchilli[6], Enricomaria Selmo[9], Andrea Spolaor[2,3], Barbara Stenni[2,3], Rita Traversi[1,2]

[1]Department of Chemistry "Ugo Schiff", University of Florence, Florence, 50019, Italy
[2]Institute of Polar Sciences of the National Research Council of Italy (ISP-CNR), 30172, Venice, Italy
[3]Department of Environmental Sciences, Informatics and Statistics of the Ca' Foscari University of Venice, Venice, 30172, Italy
[4]Laboratory of Environmental Chemistry (LUC), Paul Scherrer Institut, 5232 Villigen PSI, Switzerland
[5]National Institute of Nuclear Physics (INFN), Florence, 50019, Italy
[6]ENEA, Laboratory of Observations and Measures for the environment and climate, 00123 Rome, Italy
[7]Department of Science, Geologic Sciences section, Roma 3 University, 00154 Rome, Italy
[8]Division of Glacial Environmental Research, Korea Polar Research Institute (KOPRI), Incheon 21990, Korea
[9]Department of Chemistry, Life Sciences and Environmental Sustainability, University of Parma, Parma, 43121, Italy

[*]*Correspondence to:* Mirko Severi (mirko.severi@unifi.it)

Abstract

Ice core dating is the first step for a correct interpretation of climatic and environmental changes. In this work, we release the dating of the uppermost 197 m of the 250 m deep GV7(B) ice core (drill site, 70°41' S, 158°52'E, 1950 m a.s.l. in Oates Land, East Antarctica) with a sub-annual resolution. Chemical records of NO_3^-, MSA (methanesulfonic acid), non-sea salt SO_4^{2-}, sea-salt ions and water stable isotopes ($\delta^{18}O$) were studied as candidates for dating due to their seasonal pattern. Different procedures were tested but nssSO_4^{2-} record proved to be the most reliable on the short and long-term scale so that it was chosen for annual layer counting along the whole ice core. The dating was constrained by using volcanic signatures from historically known events as tie points thus providing an accurate age-depth relationship for the period 1179 – 2009 CE. The achievement of the complete age scale allowed to calculate the annual mean accumulation rate throughout the analyzed 197 m of the core, yielding an annually resolved history of the snow accumulation on site in the last millennium. A small, yet consistent, rise in accumulation rate ($Tr = 1.6$, $p < 0.001$) was found for the last 830 years starting around mid 18th century.

1 Introduction

Ice cores represent remarkable natural archives able to provide paleoclimatic and paleoenvironmental information, and their study is of high relevance in order to improve our understanding of the climate system. Ice cores are nowadays one of the most valuable archives to obtain long term, highly resolved records of the atmospheric composition and of the temperatures of the past, spanning from few years up to hundreds of thousands of years (Abram et al., 2013; Delmonte et al., 2002; Fischer et al., 2007; Traversi et al., 2012; Watanabe et al., 1999; Wolff et al., 2010). Antarctica and the surrounding ocean play a critical role in climate dynamics (Bertler et al., 2011), but despite the huge efforts of international programs (e.g., International Trans-Antarctic Scientific Expedition, ITASE; East Antarctic International Ice Sheet Traverse, EAIIST), a large part of the Antarctic ice sheet is still unexplored and additional cores are needed to properly reconstruct the past climate and to integrate this information in climate modeling simulations. In particular, the last millennium is a critical time frame for evaluating the more recent human-related climate change into a longer temporal context and to disentangle natural versus human impacts on climate variability, but it is still poorly investigated, particularly in Antarctica. New ice core records from Antarctica are needed for a better assessment of the surface mass balance (SMB) of the Antarctic continent, which is highly relevant to understand its role in sea-level rise in recent decades and in the near future (DeConto and Pollard, 2016; Krinner et al., 2007). Spatial coverage of climatic observation in Antarctica and the Southern Ocean is still poor (Jones et al., 2016; Neukom et al., 2018) and ice core records have the potential to investigate past SMB beyond the instrumental and satellite period. Recently, Thomas et al., (2017) investigated the Antarctic snow accumulation variability over the last millennium at regional scale using a large number of snow accumulation records, grouped and assigned to different regional Antarctic areas and compared them with modeled SMB.

In the framework of the Programma Nazionale di Ricerche in Antartide (PNRA) project "IPICS – 2kyr-IT", representing the Italian contribution to the project "The IPICS 2k Array: a network of ice core climate and climate forcing record for the last two millennia", the latter being one of the four topics of the International Partnerships in Ice Core Sciences (IPICS), several drillings have been carried out in the Oates Coast, East Antarctica. In this framework the site named GV7 (Figure 1) was chosen to retrieve ice cores covering at least 1000 yr of climatic and environmental history of this area of Antarctica. The drillings were accomplished through a bilateral Italy – South Korea collaboration, during the 2013/2014 Antarctic summer.

One of the most critical aspect of the study of the ice core records is the dating of each ice layer, which is fundamental to put the records into a temporal scale. Different methods were developed since the second half of the last century (Hammer, 1980) including the identification of seasonal pattern in chemical and physical records (Alley et al., 1997; Cole-Dai et al., 1997; Extier et al., 2018; Sigl et al., 2016), ice flow models and identification of temporal horizons such as volcanic eruptions that cause spikes in the acidity of an ice layer and/or trace elements concentration (Castellano et al., 2005; Igarashi et al., 2011; Winstrup et al., 2012, 2019).

Here, we focused on the identification of seasonal patterns in the ionic and isotopic composition of the core, the latter being one of the most reliable and extensively used method used to date many ice cores. Since $\delta^{18}O$ in falling snow varies with

seasons (Dansgaard, 1964), showing maxima in summer and minima in winter, it is possible to identify an annual cycle in $\delta^{18}O$ which is useful in the dating of a core. A similar annual pattern with either summer or winter maxima is found in both major sea salt and non-sea salt ions measured in ice cores and their records have been used in ice core dating (e.g. nitrate, MSA and the non-marine fraction of the sulphate ($nssSO_4^{2-}$); Pasteris et al., 2014; Piccardi et al., 1994; Stenni et al., 2002; Udisti, 1996). Methanesulphonic acid (MSA) and $nssSO_4^{2-}$ mainly arise from the atmospheric oxidation of their precursor dimethyl sulfide (DMS), which in turn is produced by metabolic activities of marine phytoplanktonic species (Stefels et al., 2007). The strong seasonality of DMS production leads to an analogous seasonal pattern of $nssSO_4^{2-}$ and MSA with the highest concentration peaks during the phytoplanktonic bloom, occurring in austral spring-summer (November-March) (Becagli et al., 2012).

Unlike MSA, which only arises from marine DMS (Gondwe et al., 2003), $nssSO_4^{2-}$ is formed also from the oxidation in the troposphere of SO_2, emitted during explosive volcanic eruptions, to sulphuric acid (Delmas et al., 1985). These acidic components, thanks to tropospheric and stratospheric circulation (Delmas et al., 1985) could be deposited in polar regions during a period of 2-3 years after the event (Sigl et al., 2015) and their signal is superimposed over the biogenic background of the $nssSO_4^{2-}$. The identification of such volcanic signatures in ice core records is commonly used to synchronize ice core timescales (Severi et al., 2007, 2012; Winski et al., 2019) and widely used to assign an absolute date to ice layers in a core (Castellano et al., 2005; Sigl et al., 2013) in conjunction with the annual layer counting.

A similar seasonality (with a maximum in the austral summer) is also observed in the nitrate concentration throughout the year. As one of the most abundant ions found in the cores (Legrand et al., 1999), nitrate is considered the final sink of atmospheric NO_x and due to its interaction with the main oxidant cycles in the atmosphere, it is considered one of the potential markers to reconstruct the oxidizing capacity of the past atmosphere (e.g. Dibb et al., 1998; Hastings et al., 2005). Since some of these oxidizing processes, combined with the photochemical ones, occur more intensely during summer (Erbland et al., 2013; Grannas et al., 2007) this marker can show a seasonal pattern as found in polar records (Stenni et al., 2002; Wolff, 1995). However, it must be noted that the sources, transport, and preservation of nitrate in the Antarctic snow layers are still not well understood, and that the aforementioned processes are not the only factors affecting ion concentrations in the snowpack. Deposition of HNO_3, post depositional loss and recycling of NO_3^- (e.g. Röthlisberger et al., 2002; Shi et al., 2015; Zatko et al., 2016) are all variables influencing the final nitrate concentration in ice cores. In particular, ultraviolet photolysis of nitrate and re-evaporation of HNO_3 can affect the concentration in the uppermost layers of snow, especially for sites with low snow accumulation rate (Mulvaney et al., 1998, Röthlisberger et al., 2000, 2002, Berhanu et al., 2014). Despite these processes might partially mask the seasonal pattern, nitrate records were successfully used for annual layer counting of ice cores from both hemispheres (Rasmussen et al., 2006; Thomas et al., 2007; Wolff, 2013). An opposite seasonal trend can be found for major sea-salt ions, showing late winter concentration maxima even in the innermost regions of Antarctica (Udisti et al., 2012) due to large influx of sea salt aerosol during winter months (Bodhaine et al., 1986). This seasonal pattern was observed at coastal stations (Mulvaney and Wolff, 1994; Weller et al., 2011) and Na^+ and Mg^{2+} records were successfully used in the dating of ice cores (Herron and Langway, 1979; Winski et al.,

2019). However, multiple sources contribute to the concentration of sea-salt ions in an ice core and, during winter months, the increase of sea ice extent (SIE) could in principle reduce the amount of sea spray delivered to the site. Since sea salt aerosol is generated over open water by bubble bursting (de Leeuw et al., 2011), the increase of SIE during the winter months could increase the distance from this source resulting in a loss of particles from the ocean during the long-range transport (Abram et al., 2013), potentially masking the seasonal pattern. Here we present the dating of the uppermost 197 m of the 250 m deep ice core collected at GV7, focusing on the interpretation of ion concentration records. We investigated the seasonality of the major ion markers in order to select the most reliable for annual layer counting purposes. Non-sea-salt sulfate revealed to be the most suitable parameter to point out the annual layers. For the uppermost 38 m of the ice core the dating was corroborated by the high resolution $\delta^{18}O$ record. Volcanic signatures were then used to finally constrain the dating by means of the major absolute temporal horizons provided by historically known volcanic eruptions. The obtained age scale allowed to reconstruct the snow accumulation rate variability at GV7 over the last millennium.

2 Materials and Methods

2.1 Sampling site and fieldwork

The GV7 drilling site is in the Oates Coast, a coastal area of the East Antarctica (Fig. 1). The site was chosen for its relatively high snow accumulation rate (241± 13 mm w.e. yr^{-1} over the past 50 years), the limited post depositional processes due to the reduced intensity of katabatic winds along the ice divide (Becagli et al., 2004; Frezzotti et al., 2007; Magand et al., 2004) and the excellent chemical and isotopic stratigraphies (Caiazzo et al., 2017; Frezzotti et al., 2007). Internal layers of strong radar reflectivity observed with ground-penetrating radar (GPR) are isochronous, and surveys along continuous profiles provide detailed information on the spatial variability of snow accumulation. Estimates of snow accumulation were calculated from GPR layer (dated to 1905 ± 9 AD) during the 2001-2002 ITASE expedition from 150 km north of GV7 up to Talos Dome (Frezzotti et al., 2007). Spatial distribution of snow accumulation from GPR layer upstream GV7 site shows that internal layering and surface elevation are continuous and horizontal up to 10 km from the site, revealing low ice velocity 0.3 ± 0.01 m yr^{-1}, no distortion of isochrones due to ice flow dynamics and very low snow accumulation spatial variability (less than 5%, Frezzotti et al., 2007). An extensive chemical dataset covering 7 years of deposition on site obtained from the analysis of two snow pits is already available (Caiazzo et al., 2017), as well as a detailed reconstruction of the past volcanic history (Nardin et al., 2020).

During the 2013/14 Antarctic campaign, six shallow firn cores (ranging in length between 5 and 50 m) and two intermediate firn-ice cores (87 and 250 m deep) were retrieved. The 250 m deep core (named GV7(B) was used in this study. The ice core was retrieved using an electromechanical drill (Eclipse Ice drill Instrument).

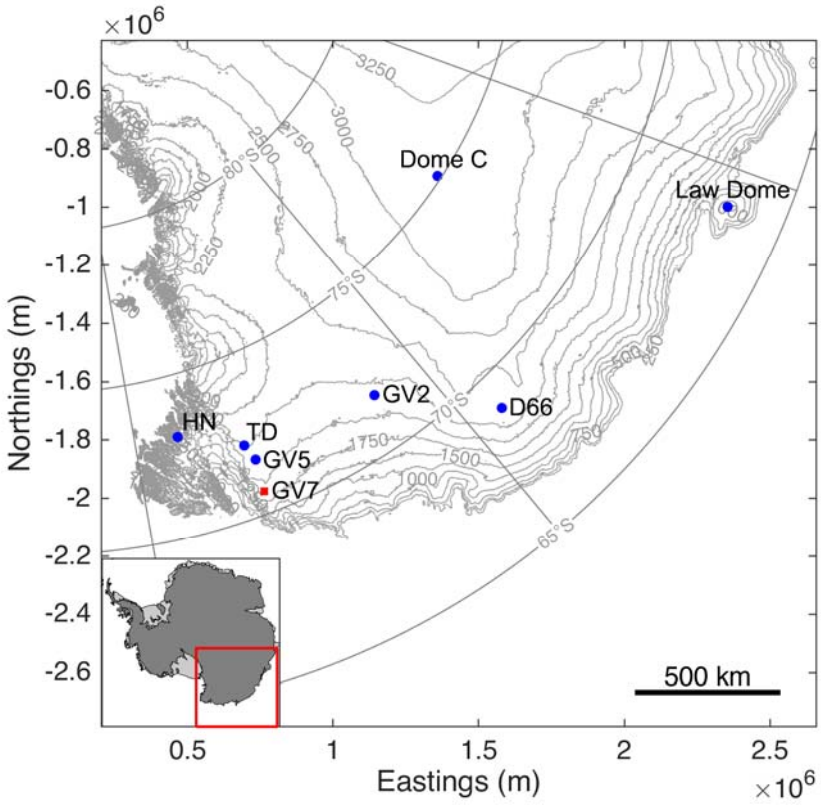

Figure 1: GV7 (70°41'17.1'' S, 158°51'48.9'' E; 1950 m a.s.l.) drilling site (red square). Hercules Nevé (HN), Talos Dome (TD), GV5, GV2, D66, Dome C and Law Dome ice core drilling sites are also shown (Greene et al., 2017; Fretwell et al., 2013)

The drilling started at 3 m from the snow surface and reached a depth of 250.2 m. Drilling fluid (Exxsol D40) was used from a depth of 80 m (close off 75 m) and added to the borehole with a tube. A stand of 4 m of fluid was found to be ideal to aid the drilling operation and to maintain an adequate quality of the core. No casing of the borehole was used to complete this shallow drilling. The Eclipse system has experienced problems during the drilling below 100 m of depth, the brittleness of the ice, breaks in the core and the presence of drilling fluids in these cracks proved to be a problem in the decontamination of the deeper sections of the core. The presence of numerous breaks prevented us to analyze the deeper part of the core and only the upper 194 meters were analyzed.

2.2 Ice core analysis

60 cm long ice core sections (cut and logged directly in field) were shipped to the EUROCOLD laboratory of the University of Milano-Bicocca (Italy) where they were cut longitudinally and transversally and distributed among different research groups. The 4x4x60 cm core strips for ionic content analysis were sealed in plastic bags, shipped frozen to the cold room of

the Department of Chemistry of the University of Florence (Italy) and stored at -20°C until the moment of analysis. Conversely, both the bag (60 cm) and the high-resolution (4 cm) samples for the isotopic analysis were melted at room temperature and transferred in 25 mL HDPE bottles at the EUROCOLD laboratory and then sent to the Ca' Foscari University of Venice and the University of Parma for the isotopic measurements.

The strips for ionic content were manually decontaminated inside the cold room of the Department of Chemistry of the University of Florence (Italy), by scraping the outermost layer of ice (approx. 1 cm) using ceramic knives to remove external contamination (Candelone et al., 1994; Chisholm et al., 1995; Tao et al., 2001, Caiazzo et al., 2016).

All decontamination procedures were carried on under a class-100 laminar flow hood and the sub samples (mean resolution of 4.5 cm) were stored inside pre-cleaned plastic vials and analyzed within a week to avoid external contamination. Some sections of the ice core were too badly damaged to be manually decontaminated, likely due to problems in the drilling operations and handling of the ice. In this case, the fractures were logged and the sample decontaminated just before the analysis by quickly submerging it three times (10 seconds the first wash then 5 seconds the remaining two) in ultra-pure water (18.2 MΩ 25°C) in order to remove the outer layer of ice. Each sub-sample was melted at room temperature under a class-100 laminar flow hood just before the analysis. The sub-samples were then analyzed for ionic content using two Ion Chromatographs operating simultaneously: a Thermo Dionex ICS-1000 for the determination of the cations (Li^+, Na^+, NH_4^+, K^+, Mg^{2+}, Ca^{2+}) and a Thermo Dionex DX-500 for anions (F^-, Formate, methanesulfonate (MS^-, referred in the text as MSA), Cl^-, NO_3^-, SO_4^{2-}). Further details about the separation methods used and the daily calibration procedures for each ion chromatographic system are described in Caiazzo et al. (2016) and Morganti et al. (2007).

Samples for isotopic analysis did not require any decontamination procedure. Bag samples (60 cm) were analyzed for $\delta^{18}O$ at the University of Parma, using a Thermo-Fisher Delta Plus Isotope-ratio Mass Spectrometer (IRMS) coupled with a HDO automatic equilibration device, following the classical water-CO_2 equilibration technique described by Epstein and Mayeda, (1953). High resolution samples (4cm) were analyzed for $\delta^{18}O$ at the Ca' Foscari University of Venice, using both the IRMS water-CO_2 equilibration technique (Thermo-Fisher Delta Plus Advantage coupled with a HDO automatic equilibration device) and the Cavity Ring-down Spectroscopy (CRDS) technique (Picarro L1102-I). The Thermo-Fisher Delta Plus and the Delta Plus advantage are both characterized by an analytical precision of 0.05‰ for $\delta^{18}O$, while the Picarro L1102-I has an analytical precision of 0.10‰ for $\delta^{18}O$. All measurements were calibrated using internal isotopic standards periodically calibrated against the certified International Atomic Energy Agency (IAEA) standards VSMOW2 and SLAP2. All the isotopic data are reported in the SMOW-SLAP δ-scale.

2.3 Major ions contribution

Chemical records of the ion markers were obtained by plotting the concentration (in μg L^{-1}) against the mid depth of the sample, logged during the decontamination procedure. The raw data set of ion concentration was kept as close as possible to the original and only extremely high concentration points (i.e. spikes in the concentration of a single ion) were discarded and attributed to external contamination. Hence, all the points above the 99th percentile for all the ions taken into account for the

dating procedure were removed; this was chosen as a fair compromise to keep high values of concentration due to particular events (e.g., volcanic eruptions) and at the same time to remove those due to possible contamination. The $nssSO_4^{2-}$ concentration was calculated by equation (1)

$$nssSO_4^{2-} = totSO_4^{2-} - 0.25 * Na^+ \quad (1)$$

where 0.253 is the average SO_4^{2-}/Na^+ ratio in sea water (Bowen, 1979), tot-SO_4^{2-} and Na^+ are the total measured concentration of the two ions respectively. We assumed that the only contribution for sodium is the sea spray aerosol (Legrand and Delmas, 1984; Maupetit and Delmas, 1992). Both in inland (Röthlisberger et al., 2002) and coastal sites (Benassai et al., 2005; Nyamgerel et al., 2020) the crustal contribution of sodium is found to be very low or negligible compared to the marine one. We calculated the terrestrial and marine contributions for Na^+ and Ca^{2+} in GV7(B) core by using a simple equation system (2) (Becagli et al., 2012; Udisti et al., 2012):

$$\begin{aligned} &tot\text{-}Na^+ = ss\text{-}Na^+ + nss\text{-}Na^+ \quad (2)\\ &tot\text{-}Ca^{2+} = ss\text{-}Ca^{2+} + nss\text{-}Ca^{2+}\\ &ss\text{-}Na^+ = tot\text{-}Na^+ - 0.562\ nss\text{-}Ca^{2+}\\ &nssCa^{2+} = tot\text{-}Ca^{2+} - 0.038\ ss\text{-}Na^+ \end{aligned}$$

where 0.562 and 0.038 represent the Na^+/Ca^{2+} w/w ratio in the crust (Bowen, 1979) and seawater (Nozaki, 1997), respectively. The non-sea salt fraction of Na^+ was found to be about 3% of tot-Na^+ on average, supporting our choice of using tot-Na^+ instead of ss-Na^+ for the calculation of $nssSO_4^{2-}$ fraction.

The $nssSO_4^{2-}$ was used to identify volcanic signatures in the GV7(B) ice core using already established methods (Castellano et al., 2004, 2005; Sigl et al., 2013; Traufetter et al., 2004) on Arctic and Antarctic ice cores. The biogenic background was calculated as the running average of the $nssSO_4^{2-}$ concentrations and its standard deviation (σ) was used to set the threshold over which a sample point was to be attributed to a volcanic eruption. Both 2σ and 3σ were used as thresholds added to the average biogenic background as described more into detail in Nardin et al. (2020).

2.4 Trace element analysis

The ice samples were analyzed with an Inductively Coupled Plasma Single Quadrupole Mass Spectrometer (ICP-qMS, Agilent 7500 series, USA) equipped with a quartz Scott spray chamber. A 120-seconds rinsing step with 2% HNO_3 (Suprapure, Romil, UK) was performed after each sample to limit any possible memory effect; the vials used for standard preparation were cleaned following the same procedure adopted for ice samples. Quantification of ^{209}Bi, ^{205}Tl and ^{238}U was performed using external calibration curves with acidified standards (2% HNO_3, Suprapure, Romil, UK) from dilution of certified IMS-102 multielemental standard (10 ppm ± 1%, Ultra scientific). The resulting external calibration curves for the

three elements showed always regression coefficients higher than 0.999. The Limit of Detection (LoD) for Tl and U was 0.001 μg L^{-1} while for Bi was 0.004 μg L^{-1}, calculated as three times the standard deviation of the blank.

2.5 Snow accumulation rate and trend analysis

On the basis of the achieved dating, the annual snow accumulation rate at the site was calculated in millimeter of water equivalent per year (mm w.e. yr^{-1}) by using the density of the core sections and a correction of the layer thickness through a thinning function . The density (in g cm^{-3}, see Figure S3) was evaluated by weighting each section of the core directly in the field after logging. The effects of layer thinning due to vertical strain rate were accounted for using a linear least squares fitting model (Dansgaard and Johnsen, 1969) considering a constant vertical strain rate on the upper 200 m and an ice thickness of 1530 m for the GV7 site. We did not consider any flow-induced layer thinning since: 1) GV7 is located on the ice divide extending from the Oates coast to Talos Dome; 2) the ice velocity at this site is very low (max. 0.3 m yr^{-1}) (Frezzotti et al., 2007); 3) the ice thickness upstream GV7 is nearly constant and thus we expect a rather constant thinning function.

Trend analysis of the accumulation rate variability was based on the calculation of breakpoints between periods with significantly different trends following Tomé and Miranda (2004). The methodology consists of a least-squares approach to compute the best continuous set of straight lines that fit a given time series, subject to a number of constraints on the minimum distance between breakpoints and, optionally, on the minimum trend change at each breakpoint. We chose a period of 150 yr as the minimum distance to identify trend at centennial scale. The choice is not objective, but complies with the high computational request for too small minimum distance and the risk of non-significance for too large minimum distance. Due to possible noise connected to local spatial variability (Frezzotti et al., 2007) at the three sites (Talos Dome, GV7 and Law Dome) we applied the procedure to a seven-year smoothed average in order to make all the cores comparable among them.

3 Results and Discussion

The relatively high snow accumulation rate at the site (well above 200 mm w.e. yr^{-1}, Frezzotti et al., 2007) allows an accurate dating of the core by counting successive snow layers, identifiable by markers having seasonal pattern and/or the identification of specific dated event, mainly as volcanic eruptions identified in the records as spikes of $nssSO_4^{2-}$ statistically higher than the biogenic background (Nardin et al., 2020).

3.1 Ice core dating procedure – upper section

A previous work on snow pit dating at the GV7 site (Caiazzo et al., 2017) revealed that $nssSO_4^{2-}$ and $\delta^{18}O$ records show the clearest seasonal pattern with in phase summer maxima. Therefore, for the uppermost section of the core (38.27 m) for which the $\delta^{18}O$ high resolution record was available, an accurate dating was obtained using $nssSO_4^{2-}$ and $\delta^{18}O$ records (Fig.

2). The seasonal maxima in the $nssSO_4^{2-}$ record were confirmed by corresponding maxima in the $\delta^{18}O$ profile.. Minor discrepancies between the two profiles were to be expected and are probably due to the slightly different depth resolution of the two series (4.5 cm and 4 cm on average for $nssSO_4^{2-}$ and $\delta^{18}O$, respectively). The reliability of this dating was further supported when compared with the volcanic signatures identified in the $nssSO_4^{2-}$ and the trace element profiles (Fig 2). The 1992 Pinatubo sulfate deposition (10.9 – 11.4 m depth) and 1964 Agung volcanic sulfate deposition (21.8 – 22.4 m) were used to constrain the dating.

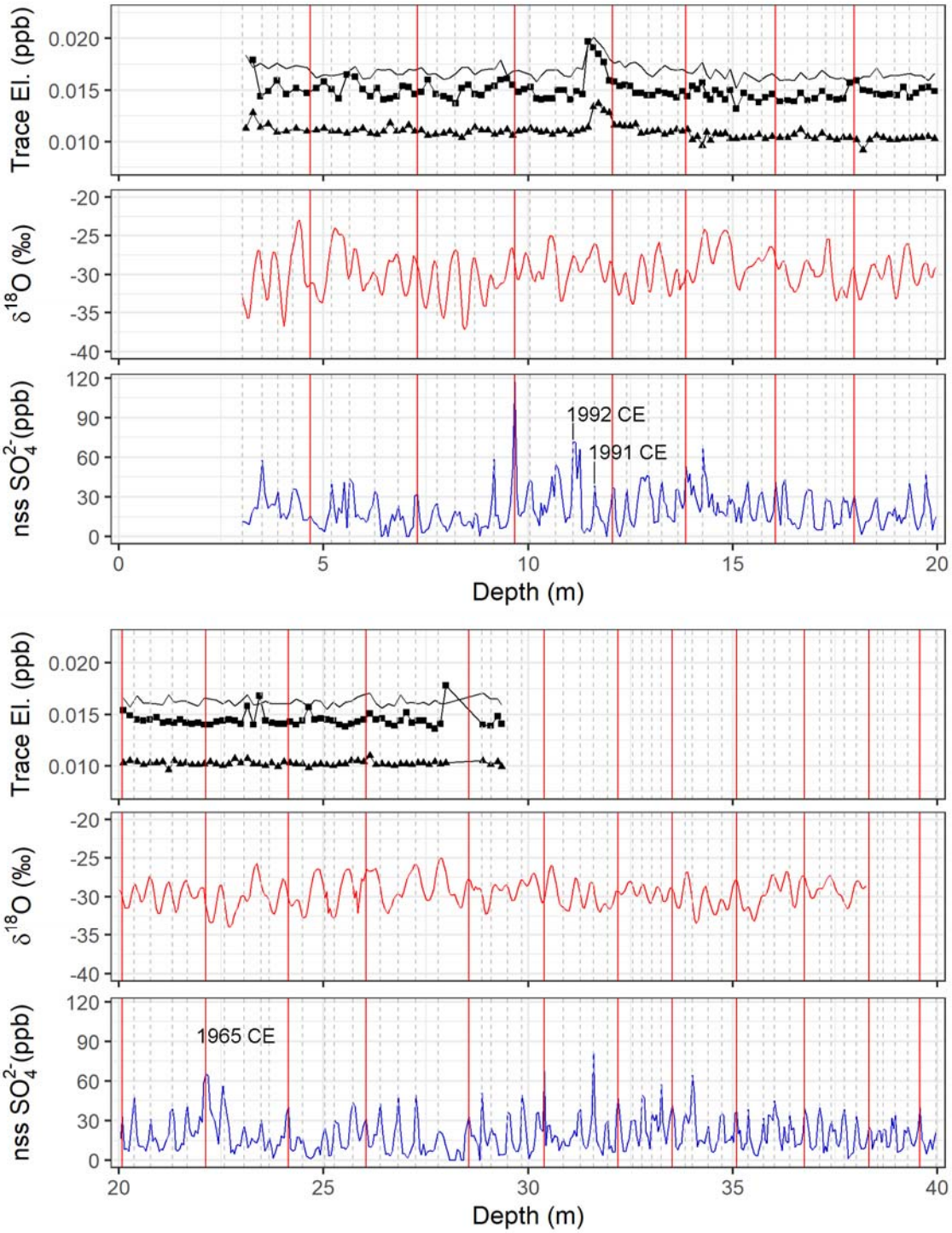

241

242

243 **Figure 2: Concentration profiles of trace elements (^{205}Tl, black solid line, ^{209}Bi, black squares, ^{238}U, black triangles), δ^{18}O (red line)**
244 **and nssSO_4^{2-} (blue line) along the uppermost 20 m (top panel) and 20-40 m intervals (bottom panel) of the GV7 (B) core. Vertical**

grey dashed lines and red lines mark annual and 5-yr intervals, respectively. The Agung and Pinatubo/Cerro Hudson volcanic signatures are also highlighted in the nssSO_4^{2-} profile with their deposition years.

As discussed in a previous work (Nardin et al. 2020), neither of these volcanic eruptions shows a prominent signal in the nssSO_4^{2-} profile and trace element records were used to support the 1992 CE tie point identification.

Trace elements deposition in polar ice caps is mainly associated with dust deposition. Evidence for anthropogenic contribution in the global trace elements deposition is well documented, such as the increase in lead depositional flux in connection with the introduction of lead containing gasoline. Specific trace elements such as Tl and Bi have been proposed to be enriched in deposition derived from volcanic eruptions (Candelone et al., 1995; Kellerhals et al., 2010). In fact, Bi, Tl and U show an increased concentration between 11.03 and 12.90 m (^{205}Tl), 11.33 and 12.62 m (^{209}Bi) and 11.03 and 13.33 m depth (^{238}U, see Fig. 2), corresponding to the 1989–1992 CE time period, according to the annual layer counting dating. Bi, Tl and U concentrations peaks seem to be not perfectly coeval with the Pinatubo/Cerro Hudson signature in the nss-sulfate profile, being recorded at a slightly higher depth with respect to nssSO_4^{2-}.This small time gap can be explained considering that dust (and therefore trace elements) deposition often occurs earlier than sulfate, as reported by Hwang et al. (2019) for the same volcanic eruption recorded in snow pits from Dome Fuji area. No clear evidence of a statistically significant increment in the ^{205}Tl, ^{209}Bi or ^{238}U levels were found in correspondence with the 1963 Agung eruption. For this section of the core, only the nssSO_4^{2-} signal was used to constrain the dating. As a conclusion, the uppermost section of the core (3.00 to 38.27 m) was dated and was found to cover the time period 2009–1920 CE. The uncertainty of this dating is discussed further below.

3.2 Ice core dating procedure – lower section

Due to the lack of high-resolution data for $\delta^{18}O$ for the deeper part of the core, only ion signatures could be used for the dating of the rest of the core. In order to highlight the seasonal character of each ion and to assess their reliability for dating purposes, we considered the concentration profile of each ion throughout the 89 years already dated in the above section. Each year was equally divided in four parts corresponding to the Antarctic seasons and roughly to the time periods January-March, April-June, July-September and October-December and bin-plots were produced (Fig. 3). In this way, we were able to point out the markers showing a clear seasonal pattern by using bin plots (Figure 3). When comparing the profile of each ion to the average calculated in the considered time interval (dashed blue line in Figure 3), all the species showed a maximum throughout the year. Anyway ,as shown in Fig. 3, the most pronounced seasonal pattern was shown by nssSO_4^{2-} with a high occurrence of low concentration points during winter months and a high occurrence of high concentration points at the beginning of the year. Typical sea-salt ions showed winter maxima, and especially Mg^{2+} (Figure 3 c), with generally higher values of concentration (up to 3.5 μg L^{-1} compared to an average of 1.7 μg L^{-1}), but in general the most populated bins in the winter and summer periods showed similar concentrations, suggesting a lack of clear seasonality.

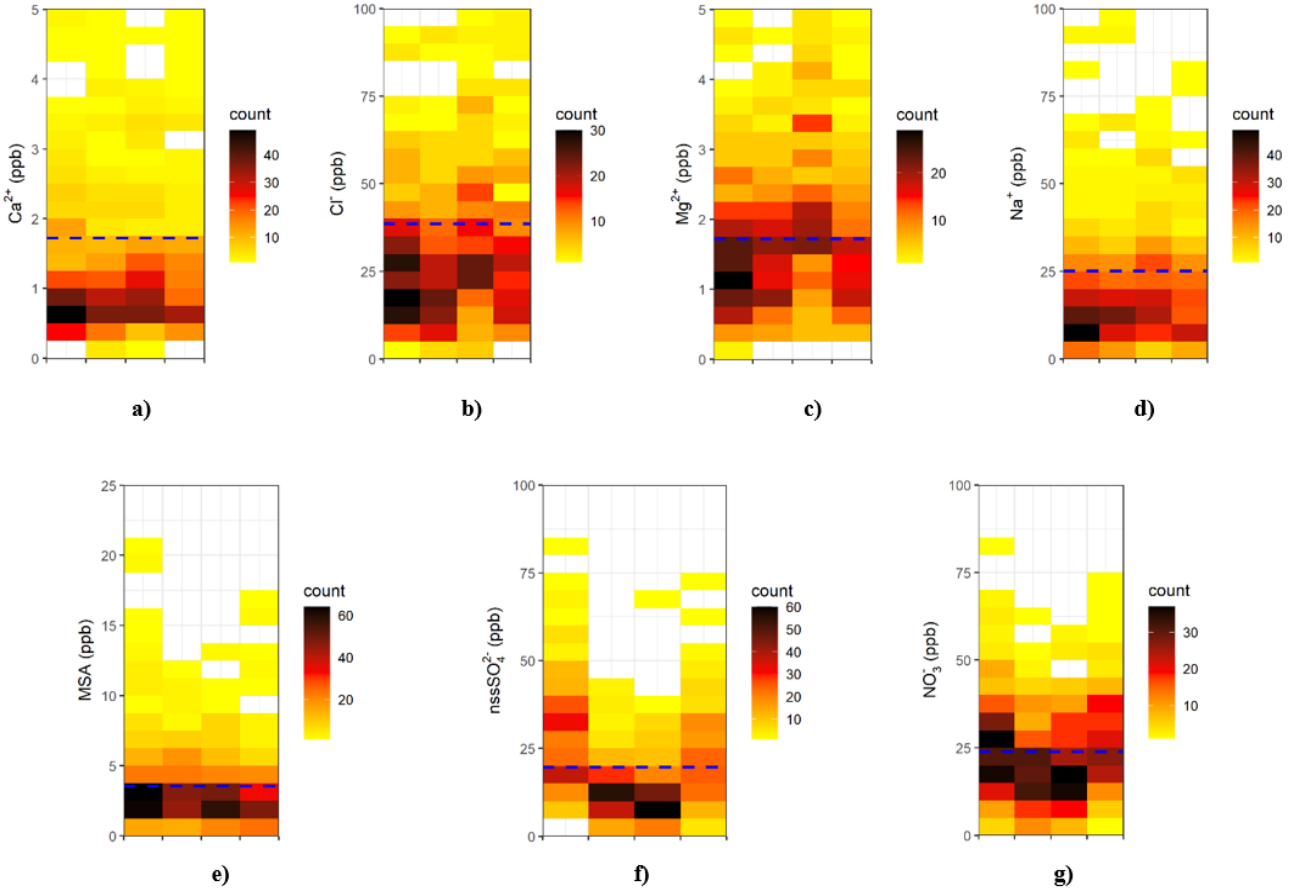

Figure 3: Seasonal variability of Ca^{2+} (a), Cl^- (b), Mg^{2+} (c), Na^+ (d), MSA (e), $nssSO_4^{2-}$ (f) and NO_3^- (g) concentrations in the GV7(B) ice core. Concentration bins are 3 "months" in width (JFM, AMJ, JAS, OND) and 5 ppb in height except for MSA levels (1 ppb) and Calcium and Magnesium (0.25 ppb).. Dashed blue lines show the average concentration of each ion in the investigated time interval.

These considerations only cover a small section of the core (approx. the 20% of its length), but as shown in Figure S1, neither Na^+ nor Mg^{2+} concentration profiles seem to show a clear annual pattern at relatively high depths and not always a maximum in the $nssSO_4^{2-}$ concentration coincide with a minimum in the other two ions concentration.

Based on the seasonality of the ionic markers (here highlighted by the bin plots), we tested for GV7(B) ice core, several dating procedures reported in literature. We tried both single-parameter and multiparametric approaches as proposed for instance by Herron and Langway (1979), Udisti (1996) and Winski et al. (2019) but $nssSO_4^{2-}$ profile solely showed the clearest seasonal signal along the whole core (Fig. S1 and S2). The dating of the core was therefore carried out with a combination of annual layer counting and the identification of volcanic signatures, both from $nssSO_4^{2-}$ profile. The known past volcanic eruptions found in other ice cores (Sigl et al., 2013, 2015, 2016; Zielinski et al., 1996) as well as a tephra layer (Narcisi et al., 2001, 2012; Narcisi and Petit, 2021) and their assigned date are reported in Table 1. The complete record of $nssSO_4^{2-}$ is reported in Figure 4 and the final age to depth relationship is shown in Figure 5. When performing annual layer

293 counting, a rigorous evaluation of the uncertainty of the dating is difficult to be accomplished and it is usually performed by
294 the algorithm used to identify each annual layer (Sigl et al., 2016; Winski et al., 2019) and/or by considering the uncertainty
295 of the dating of different ice cores used as reference (Winski et al., 2019). In this work we estimated the uncertainty of the
296 annual layer counting as the sum of the layer uncertainties highlighted in the dating procedure, estimated to be 0.5 ± 0.5
297 years (Rasmussen et al., 2006). The uncertainty was estimated between the two consecutive known volcanic signatures in the
298 core, dated with an uncertainty of ±1 year from the recorded eruption due to the time needed to reach Antarctica.

299 The same level of uncertainty was assigned to the missing sections of the core, where the number of years present was
300 estimated using the average ratio between the number of years and related depth interval calculated in 10 yr time-span before
301 and after the break. Uncertainty levels are reported in Table 2; the relatively higher number of uncertain layers in the lower
302 section of the core is due to missing ice (whose percentage is reported in Table 2 as well) that led to a non-continuous profile
303 and to a lower resolution of the core. There are fewer major eruptions in this section of the core (Table 1) and as they are
304 further apart, the uncertainty becomes larger.

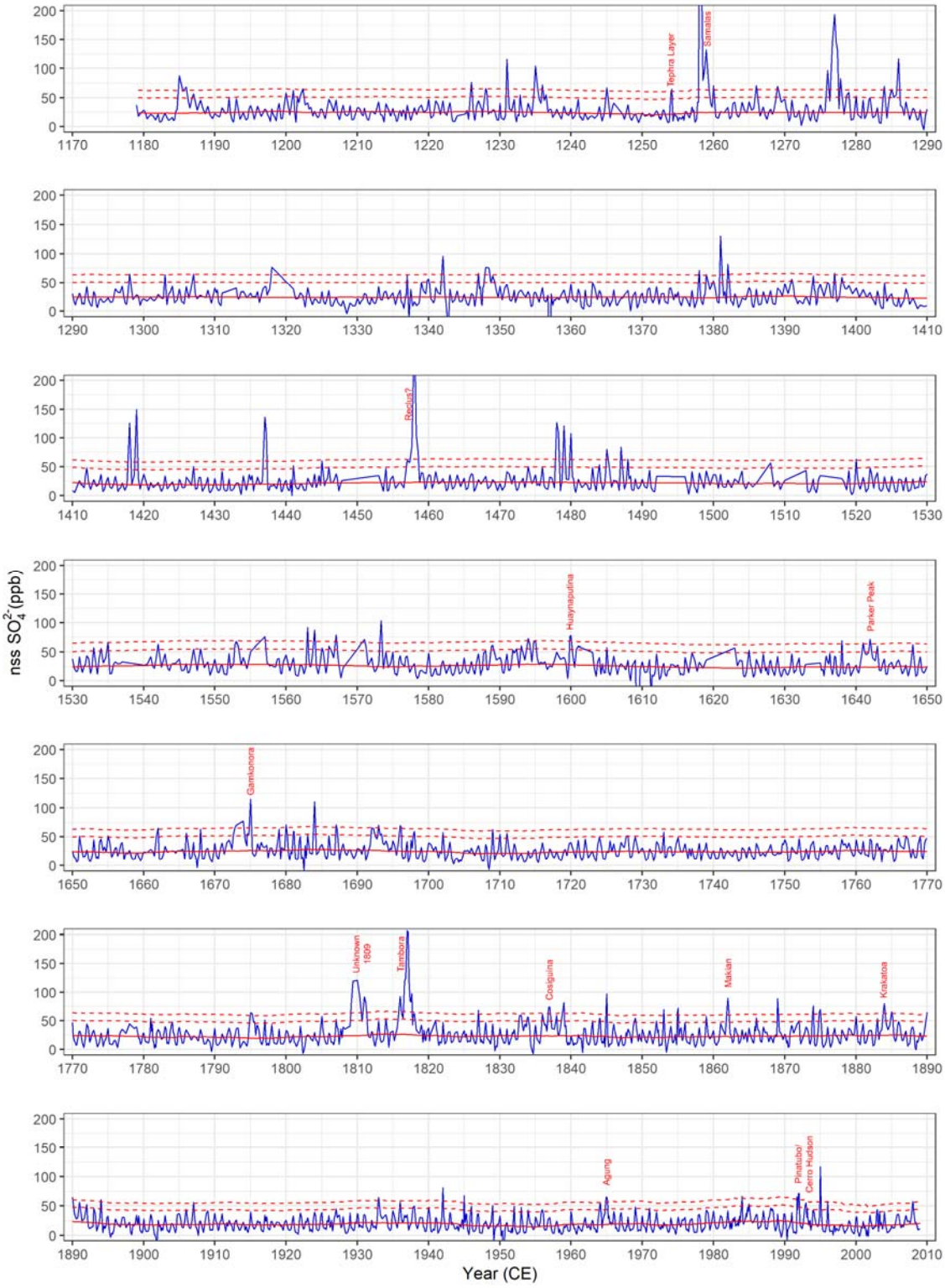
nss SO_4^{2-} (ppb)
Tephra Layer
Sanralas
Reclus?
Huaynaputina
Parker Peak
Ganikonora
Unknown 1809
Tambora
Cosiguina
Makian
Krakatoa
Agung
Pinatubo/ Cerro Hudson
Year (CE)

305

306 **Figure 4: GV7(B) nssSO_4^{2-} profile plotted on the age scale produced in this paper.. Biogenic background (solid red) and thresholds**
307 **used to identify the volcanic signatures (2σ and 3 σ, dashed red) are also reported.**

308

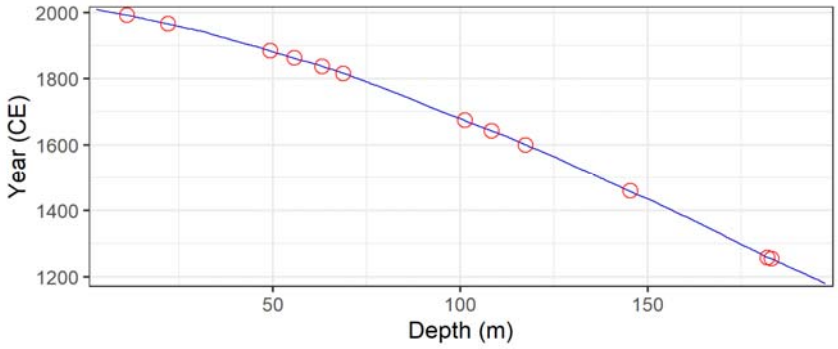

309

310 **Figure 5: age-depth relationship for the GV7(B) ice core. Temporal horizons used as constraints in the dating procedure are**
311 **highlighted with red circles.**

312

313 **Table 1: known past volcanic eruptions used in the dating of the core**

314

315

Volcano	Depth (m)		Historical eruption date (start) Year (CE)	Assigned deposition date Year (CE)
	Interval	Max. nssSO_4^{2-}		
Pinatubo/Cerro Hudson	10.91 – 11.42	11.10	1991	1992
Agung	21.82 – 22.43	22.12	1963	1965
Krakatoa	49.01 – 49.53	49.35	1883	1884
Makian	55.55 – 56.12	55.75	1861	1863
Cosiguina	63.05 – 63.64	63.27	1835	1837
Tambora	68.16 – 69.18	68.75	1815	1816
Gamkonora	100.90 – 101.61	101.25	1673	1675
Parker Peak	108.18 – 108.77	108.39	1641	1642
Huaynaputina	117.38 – 117.62	117.48	1600	1600
Reclus?	145.05 – 145.61	145.41	1460	1460
Samalas	181.40 – 182.12	181.86	1257	1258
Tephra Layer	182.07 – 183.14	183.07	1253	1254

316

Table 2: Uncertainty of the GV7(B) ice core dating in the depth intervals comprised between two consecutive volcanic eruptions. Missing sections of the core, as percentage, are also reported

GV7(B) section (m)	Missing ice (%)	Local max in $nssSO_4^{2-}$	Annual Layers		Duration (yrs)	Counting Error	
			Certain	Uncertain		Abs (yrs)	Percentage
3.00 – 11.10	0.37	17	17	0	17	-	-
11.10 - 22-12	0.18	28	26	2	27	1	3.7
22.12 – 49.35	0.48	86	76	10	81	5	6.2
49.35 – 55.75	0.31	27	21	2	22	1	4.5
55.75 – 68.75	0.38	50	42	12	48	6	12.5
68.75 – 101.25	2.15	146	136	10	141	5	3.5
101.25 – 108.39	2.46	34	31	2	32	1	3.1
108.39 – 117.48	2.53	44	37	8	41	4	9.8
117.48 – 145.41	8.80	142	133	18	142	9	6.3
145.41 – 181.86	3.76	200	188	24	200	12	6.0
181.86 –183.07	0.82	4	4	0	4	-	-
183.07 – 197.00	0.18	75	69	12	75	6	8.0

3.3 Mean Snow Accumulation Rate evaluation

A mean accumulation rate of 242 ± 71 mm w.e. yr^{-1} for the period 2008 – 2013 CE, was found at the same site by Caiazzo et al. (2017). This value is very close to the accumulation rate over the previous 35 years made by Magand et al. (2004) using atomic bomb horizon markers (241 ± 13 mm w.e. yr^{-1} from 1965 to 2000 CE). Frezzotti et al. (2007) reported an accumulation of 252 ± 104 mm w.e. yr^{-1} for the period 2001 – 2004 CE using snow stakes farm measurements. For a longer time period (1854 – 2004 CE) a mean accumulation of 237 mm w.e. yr^{-1} was assessed using atomic bomb markers and $nssSO_4^{2-}$ spikes from known volcanic events as age markers (Frezzotti et al, 2007).

The mean GV7(B) accumulation rate here calculated for the 1965 – 2000 CE and 1854 – 2004 CE time intervals (242 ± 57 mm w.e. yr^{-1} and 233 ± 64 mm w.e. yr^{-1}, respectively) are in good agreement with those found in the snow pits, stake measurements and shallow ice cores previously reported. Considering the full ice core record (195 m), covering the 1179 – 2009 CE time interval, the mean snow accumulation resulted to be 205 ± 63 mm w.e. yr^{-1}, lower than the one previously measured for the last centuries.

The comparison between GV7(B) and the GV7 ITASE records (Fig. 6) highlights a similar variability in annual snow accumulation especially in the period ranging from 1900 to 2001 CE where the linear correlation between the two cores is high and significant ($R=0.42$, $p<0.0001$). On the other hand, if we consider also part of the 18th century, the correlation decreases ($R=0.3$ $p<0.0002$) due to few inconsistencies between 1880 and 1850 CE, probably caused by the uncertainty of the two different age scales.

In order to remove the possible noise due to post depositional processes (e.g. sastrugi) (Frezzotti et al., 2007) and to reduce the error due to the underestimation (overestimation) of the yearly accumulation rate, a stacked record was obtained by combining the available records: a snow pit covering the 2008 – 2013 CE time interval; GV7(B) core (1079 – 2009 CE), stake measurements (2001 – 2003 CE) and GV7 ITASE core (1849 – 2001 CE). The new stacked record (Figure 6) can give valuable information on snow accumulation trend in the Antarctic region through comparison with other ice cores drilled in the same sector. In the East Antarctic region, facing the Southern Indian Ocean, only three ice core records of snow accumulation cover a period longer than three centuries: GV7 stacked (1179 – 2013 CE, this paper), Law Dome (-22 – 2012 CE; Roberts et al., 2015) and Talos Dome (1217 – 2010 CE; Stenni et al., 2001, Thomas et al., 2017). Other cores (D66, GV5, GV2, HN) have been drilled but their records cover less than 300 years (Frezzotti et al., 2013; Thomas et al., 2017). Law Dome (DSS) is a site close to the Southern Ocean (100 km from the shoreline) at about 1400 m a.s.l. with a mean accumulation rate of 740 mm w.e. yr^{-1} over the last two millennia (van Ommen et al., 2004). We must take into account that DSS site is about 1900 km west of GV7. Talos Dome is located at 2316 m a.s.l and 250 km southern inland of GV7, with a long-term accumulation rate of 80 mm w.e. yr^{-1} over the last 800 years (Stenni et al., 2001). The comparative analysis of the last 800 years of these three records shows a significant trend in the accumulation rate record at GV7 and Law Dome (Table 3), with a high increase in the accumulation rate at GV7 and a slight increase at Law Dome (47 and 20 mm w.e., ~23% and ~2% of the mean accumulation over 800 years, respectively). On the other hand, no significant trend at Talos Dome can be pointed out (Table 3). Frezzotti et al. (2013) analyzed 67 records from the entire Antarctic continent over the last 800 years to assess the temporal variability of accumulation rates. The temporal and spatial variability of the records highlights that snow accumulation changes over most of Antarctica are statistically negligible and do not exhibit a clear long-term trend. However, an increase in accumulation rate higher than 10% was observed in coastal and slope regions, in agreement with our findings for the GV7 site. The breaking point analysis (Fig. 7) showed that each site is characterized by multi-centennial time intervals with different trends. GV7 shows a low accumulation rate from the beginning of record (1200 CE) to the middle of the 14th century; a similar decrease had been already observed at Law Dome (Roberts et al., 2015) and at Talos Dome (Stenni et al. 2001) (Fig. 7). GV7 accumulation rate record shows an increase from the middle 18th century up to now; the same trend can be observed for Talos Dome (Table 3), whereas at Law Dome such an increase starts about a century later. Previous studies regarding the Talos Dome – GV7 area, pointed out a century-scale variability with a slight increase (of a few percent) in accumulation rates over the last two centuries, particularly since the 1960s, compared with the period 1816 – 1965 CE (Frezzotti et al., 2007, 2013). At GV7 the observed increase in accumulation during the last 250 years is

367 greater than the observed range for the previous 600 years (Fig. 7). For Talos Dome, Stenni et al. (2001) pointed out a
368 decrease during part of the Little Ice Age, 1217 – 1996 CE, followed by an increase of about 11% in accumulation during the
369 20th century. On the other hand, Roberts et al. (2015) found out that the two thousand years (22 BCE to 2012 CE) record at
370 Law Dome showed no long-term trend in snow accumulation rates, although several anomalous periods of accumulation rate
371 can be spotted in the record. The accumulation variability observed at Law Dome was associated with both ENSO and IPO
372 (Roberts et al., 2015; Vance et al., 2015), which influence the meridional component of the large-scale circulation (van
373 Ommen and Morgan, 2010; Roberts et al., 2015; Vance et al., 2015). Thomas et al. (2017), using 79 annually resolved snow
374 accumulation records, showed that snow accumulation for the total Antarctic continent increased since 1800 AD and the
375 annual snow accumulation during the most recent decade (2001 – 2010) is higher than the annual average at the start of the
376 19th century. The Antarctic Peninsula is the only region where both the most recent 50- and 100- year trends are larger than
377 the observed range for the past 300 years. This result is coherent with the trend increase highlighted in this paper by breaking
378 point analysis applied to the GV7 stacked record. Although in different periods some common trends are evident in the
379 records, there is not a clear agreement among all the accumulation records. This can be explained by the different origin and
380 atmospheric pathways of the air masses responsible of the precipitations at the three sites, despite being located in the same
381 macro region of East Antarctica. Indeed, precipitations over the GV7 area are related to storms coming from the Southern
382 Indian Ocean (Caiazzo et al., 2017) as for Law Dome, whereas the precipitation at Talos Dome is coming only for 50% from
383 the Southern Indian Ocean and the remaining from the Ross Sea (Sodemann and Stohl, 2009; Scarchilli et al. 2011).

384
385
386
387
388

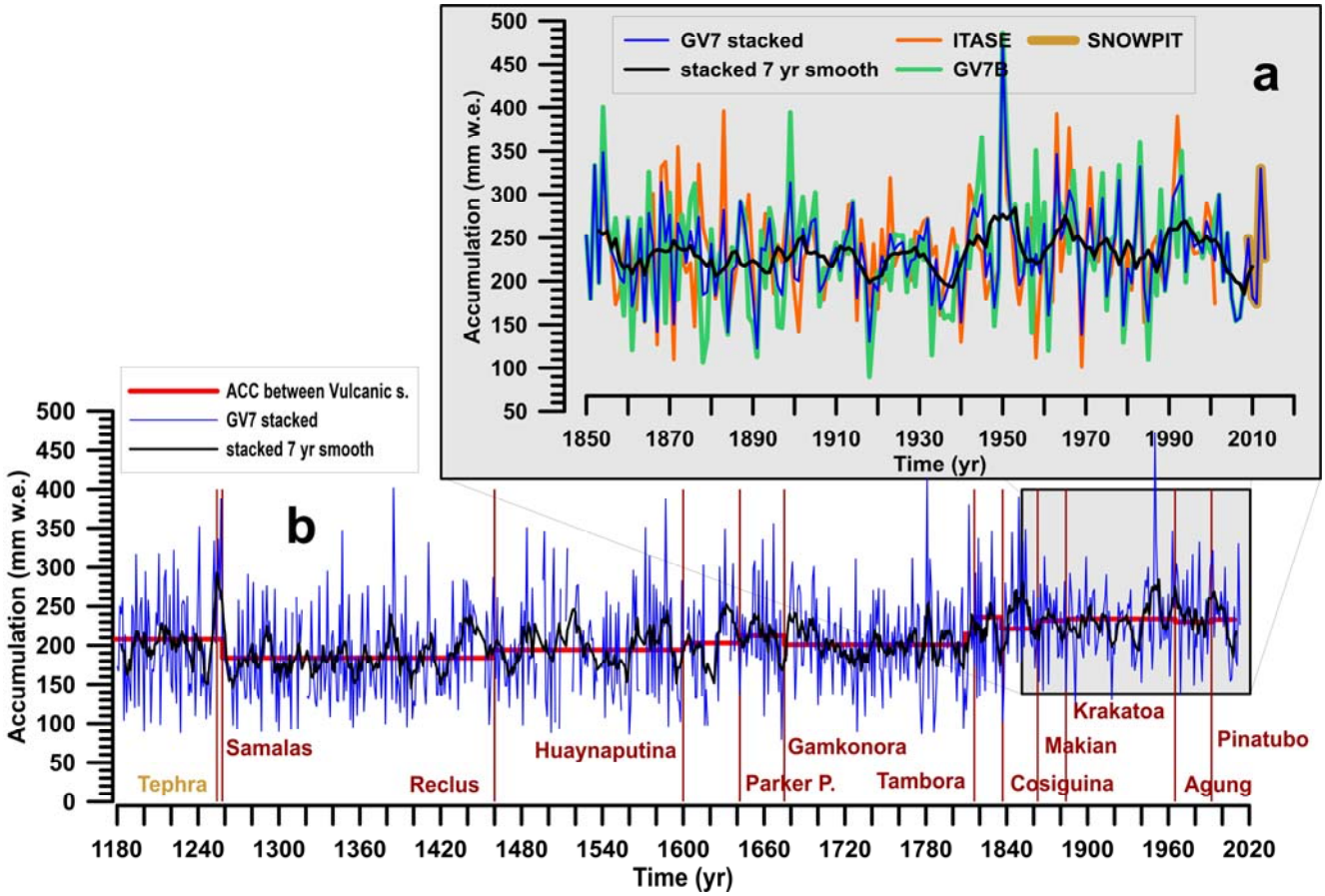

Figure 6: a) Time series from 1840 to 2020 CE of the GV7 snowpit (2008 – 2013 CE, gold line); the ITASE core (1849 – 2001 CE, orange line) and the GV7(B) core (1179 – 2009 CE, green line). Blue and black lines highlight the stacked record, obtained integrating the snowpit, ITASE and GV7(B) core records, and its smoothing at 7 years, respectively. b) GV7 stacked time record (1179 – 2013 CE) with seven-years smoothing average (black line). Red vertical bars highlight volcanic eruption horizons and red line shows average accumulation rate between different volcanic events.

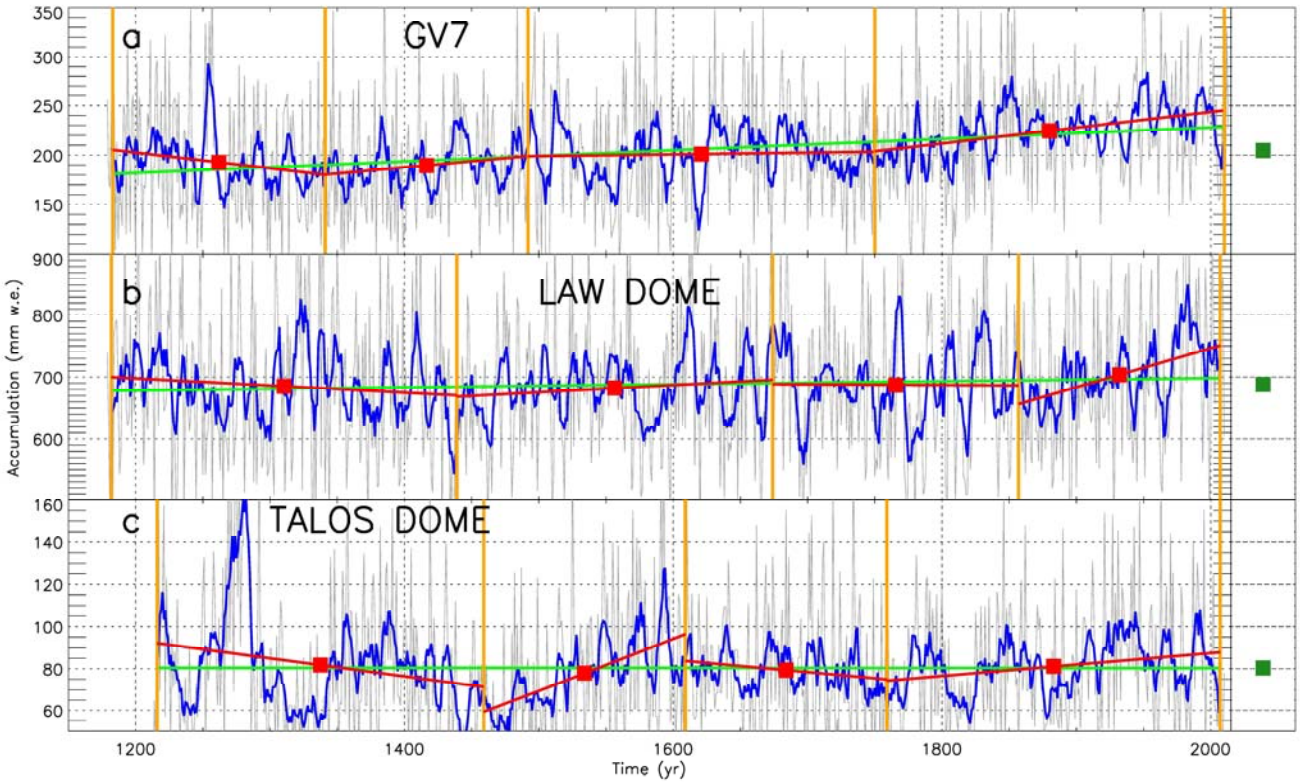

Figure 7: a) GV7 stacked record (gray line) with its seven yr smoothing average (blue line); green line represents trend for the 1179-2013 CE record. Yellow vertical bars show breaking points (1183 CE, 1341 CE, 1492 CE, 1750 CE and 2010 CE) calculated following Tomé and Miranda (2004). Red lines and filled squares show partial trends and mean accumulation (with standard deviation error bars) for each sub-period defined by breaking points. Green filled square with error bar highlights mean accumulation at the site and its standard deviation, respectively, for the whole period (1179-2013 CE). b) Same as a) but for Law Dome ice core for the period 1179-2013 CE with breaking points at 1182 CE, 1439 CE, 1674 CE, 1857 CE and 2007 CE. c) Same as a) but for Talos Dome ice core for the period 1216-2010 CE with breaking points at 1216 CE, 1459 CE, 1609 CE, 1759 CE and 2007 CE.

Table 3: Values of trend (Tr, mm w.e./decade), associated significance (p-value) and mean accumulation rate (M, mm w.e. yr^{-1}) for GV7 stacked, Law Dome and Talos Dome records smoothed using a 7-year running average. The time intervals reported in the table correspond to the different periods defined by breaking points analysis.

GV7 stacked	**1183-2010** Tr=+0.6 ($p < 0.001$) M=205	**1183-1341** Tr=-1.6 ($p < 0.001$) M=193	**1341-1492** Tr=1.2 ($p < 0.001$) M=190	**1492-1750** Tr=0.2 (No sign.) M=201	**1750-2010** Tr=1.6 ($p < 0.001$) M=224
LAW DOME	**1183-2007** Tr=-0.3 ($p < 0.001$) M=688	**1183-1439** Tr=-1.1 ($p < 0.01$) M=685	**1439-1674** Tr=1.1 ($p < 0.01$) M=682	**1674-1857** Tr=-0.1 (No sign) M=687	**1857-2007** Tr=6.3 ($p < 0.001$) M=704
TALOS DOME	**1216 -1996** No trend M=80	**1217-1459** Tr=-0.9 ($p < 0.001$) M=82	**1459-1609** Tr=2.5 ($p < 0.001$) M=78	**1609-1759** Tr=-0.6 ($p < 0.001$) M=79	**1759-2007** Tr=0.5 ($p < 0.001$) M=81

4 Conclusions

In this work, we used the chemical stratigraphies obtained from the analysis of about 3500 discrete samples from the GV7(B) ice core to accurately date the core with a sub-annual resolution. $\delta^{18}O$ high resolution record was compared to $nssSO_4^{2-}$ profile showing negligible discrepancies. The two records were used to achieve a reliable dating of the uppermost section of the core (approx. 40 m, covering the time period between 1920 and 2009 CE).

For the deeper section of the core, different strategies were tested and compared, namely single-parameter and multi-parametric approaches by considering seasonal markers to accomplish an annual layer counting. Upon these tests, $nssSO_4^{2-}$ profile was chosen for the dating of the core because of its clearer and better-preserved seasonal pattern all along the ice core, even at higher depths, where the temporal resolution becomes lower due to the thinning of the ice layers. An accurate annual layer counting was applied, and the volcanic signatures identified in the GV7(B) ice core were used as temporal horizons and tie points in the dating procedure. In this way, an accurate dating of the core with a sub-annual resolution for the uppermost 197 m was obtained. Unfortunately, beyond the depth of 197 m, the ice core was strongly damaged and thus

heavily contaminated from the drilling fluid also in the inner part. The GV7(B) chronology covers the 1179-2009 CE period. The average annual snow accumulation for this period is 205 mm w.e. This value was compared with already available records from the same site and different cores drilled in the same region (Law Dome and Talos Dome). A similar accumulation rate was found when comparing it with another core drilled on the same site as part of the ITASE drilling campaign, with a particularly good agreement during the last 40 years. When considering the general trend of the accumulation throughout the years, an increase was found since middle 18^{th} century covered by the GV7(B) core. This increasing trend was observed also at other slope coastal sites. Although the data here presented only cover the last 830 years, the number of cores that are able to cover the same time period is still scarce, therefore the present study could significantly contribute to the long-term assessment of the surface mass balance in this area.

Data Availability

The GV7(B) chronology, volcanic tie points, uncertainty of the age scale and supporting data sets will be made available upon request to the corresponding author.

Author contributions

RN, MS, AA, SB, LC, SH and RT took care of the IC sample decontamination and/or ion chromatographic analysis and performed the annual layer counting. FB, IK and AS analysed the trace elements content. GD, BS and ES measured water stable isotopes. VC, MF, CS, BMN and MP took care of the accumulation rate analysis. RN, LC, SB, MS and RT wrote the paper with inputs from all authors.

Competing interest

The authors declare that they have no conflict of interest.

Acknowledgment

This research was financially supported by the MIUR (Italian Ministry of University and Research) - PNRA (Italian Antarctic Research Programme) through the IPICS-2kyr-It project (International Partnership for Ice Core Science, reconstructing the climate variability for the last 2kyr, the Italian contribution). The IPICS-2kyr-It project is carried out in cooperation with KOPRI (Korea Polar Research Institute, grant No. PE21100).

The fellowship personnel involved in the analysis of the GV7(B) core, and the laboratory equipment was partially funded by Fondazione Cassa di Risparmio di Firenze, MIUR-PNRA IPICS-2kyr-Italia (PNRA 2009/A2.09) MIUR-PNRA "BE-OI" (PNRA16 00124) and "3D" (PNRA16 00212) projects and MIUR-PRIN 2017 "AMICO".

References

Abram, N. J., Wolff, E. W. and Curran, M. A. J.: A review of sea ice proxy information from polar ice cores, Quaternary Science Reviews, 79, 168–183, https://doi.org/10.1016/j.quascirev.2013.01.011, 2013.

Alley, R. B., Shuman, C. A., Meese, D. A., Gow, A. J., Taylor, K. C., Cuffey, K. M., Fitzpatrick, J. J., Grootes, P. M., Zielinski, G. A., Ram, M., Spinelli, G. and Elder, B.: Visual-stratigraphic dating of the GISP2 ice core: Basis, reproducibility, and application, Journal of Geophysical Research: Oceans, 102(C12), 26367–26381, https://doi.org/10.1029/96JC03837, 1997.

Becagli, S., Proposito, M., Benassai, S., Flora, O., Genoni, L., Gragnani, R., Largiuni, O., Pili, S. L., Severi, M., Stenni, B., Traversi, R., Udisti, R. and Frezzotti, M.: Chemical and isotopic snow variability in East Antarctica along the 2001/02 ITASE traverse, Annals of Glaciology, 39, 473–482, https://doi.org/10.3189/172756404781814636, 2004.

Becagli, S., Scarchilli, C., Traversi, R., Dayan, U., Severi, M., Frosini, D., Vitale, V., Mazzola, M., Lupi, A., Nava, S. and Udisti, R.: Study of present-day sources and transport processes affecting oxidised sulphur compounds in atmospheric aerosols at Dome C (Antarctica) from year-round sampling campaigns, Atmospheric Environment, 52, 98–108, https://doi.org/10.1016/j.atmosenv.2011.07.053, 2012.

Benassai, S., Becagli, S., Gragnani, R., Magand, O., Proposito, M., Fattori, I., Traversi, R. and Udisti, R.: Sea-spray deposition in Antarctic coastal and plateau areas from ITASE traverses, Annals of Glaciology, 41, 32–40, https://doi.org/10.3189/172756405781813285, 2005.

Berhanu, T. A., Meusinger, C., Erbland, J., Jost. R., Bhattacharya, S. K., Johnson, M. S., Savarino, J.: Laboratory study of nitrate photolysis in Antarctic snow. II. Isotopic effects and wavelength dependence, Journal of Chemical Physics 140, 244306 https://doi.org/10.1063/1.4882899, 2014

Bertler, N. A. N., Mayewski, P. A. and Carter, L.: Cold conditions in Antarctica during the Little Ice Age - Implications for abrupt climate change mechanisms, Earth and Planetary Science Letters, 308(1–2), 41–51, https://doi.org/10.1016/j.epsl.2011.05.021, 2011.

Bodhaine, B. A., Deluisi, J. J., Harris, J. M., Houmere, P. and Bauman, S.: Aerosol measurements at the South Pole, Tellus B, 38 B(3–4), 223–235, https://doi.org/10.1111/j.1600-0889.1986.tb00189.x, 1986.

Bowen, H. J. M.: Environmental chemistry of the elements, Academic Press, London., 1979.

Caiazzo, L., Becagli, S., Frosini, D., Giardi, F., Severi, M., Traversi, R. and Udisti, R.: Spatial and temporal variability of snow chemical composition and accumulation rate at Talos Dome site (East Antarctica), Science of the Total Environment, 550, 418–430, https://doi.org/10.1016/j.scitotenv.2016.01.087, 2016.

Caiazzo, L., Baccolo, G., Barbante, C., Becagli, S., Bertò, M., Ciardini, V., Crotti, I., Delmonte, B., Dreossi, G., Frezzotti, M., Gabrieli, J., Giardi, F., Han, Y., Hong, S. B., Hur, S. D., Hwang, H., Kang, J. H., Narcisi, B., Proposito, M., Scarchilli, C., Selmo, E., Severi, M., Spolaor, A., Stenni, B., Traversi, R. and Udisti, R.: Prominent features in isotopic, chemical and

485 dust stratigraphies from coastal East Antarctic ice sheet (Eastern Wilkes Land), Chemosphere, 176, 273–287,
486 https://doi.org/10.1016/j.chemosphere.2017.02.115, 2017.
487 Candelone, J.-P., Hong, S. and Boutron, C. F.: An improved method for decontaminating polar snow or ice cores for heavy
488 metal analysis, Analytica Chimica Acta, 299(1), 9–16, 1994.
489 Candelone, J.-P., Bolshov, M. A., Rudniev, S. N., Hong, S. and Boutron, C. F.: Bismuth in recent snow from Central
490 Greenland: Preliminary results, Atmospheric Environment, 29(15), https://doi.org/10.1016/1352-2310(95)00058-7, 1995.
491 Castellano, E., Becagli, S., Jouzel, J., Migliori, A., Severi, M., Steffensen, J. P., Traversi, R. and Udisti, R.: Volcanic
492 eruption frequency over the last 45 ky as recorded in Epica-Dome C ice core (East Antarctica) and its relationship with
493 climatic changes, in Global and Planetary Change, vol. 42, pp. 195–205, https://doi.org/10.1016/j.gloplacha.2003.11.007, ,
494 2004.
495 Castellano, E., Becagli, S., Hansson, M., Hutterli, M., Petit, J. R., Rampino, M. R., Severi, M., Steffensen, J. P., Traversi, R.
496 and Udisti, R.: Holocene volcanic history as recorded in the sulfate stratigraphy of the European Project for Ice Coring in
497 Antarctica Dome C (EDC96) ice core, Journal of Geophysical Research D: Atmospheres, 110(6), 1–12,
498 https://doi.org/10.1029/2004JD005259, 2005.
499 Chisholm, W., Rosman, K. J. R., Boutron, C. F., Candelone, J. P. and Hong, S.: Determination of lead isotopic ratios in
500 Greenland and Antarctic snow and ice at picogram per gram concentrations, Analytica Chimica Acta, 311(2), 141–151,
501 https://doi.org/10.1016/0003-2670(95)00181-X, 1995.
502 Cole-Dai, J., Mosley-Thompson, E. and Thompson, L. G.: Annually resolved southern hemisphere volcanic history from two
503 Antarctic ice cores, Journal of Geophysical Research Atmospheres, 102(14), 16761–16771,
504 https://doi.org/10.1029/97jd01394, 1997.
505 Dansgaard, W.: Stable isotopes in precipitation, Tellus, 16(4), 436–468, https://doi.org/10.1111/j.2153-3490.1964.tb00181.x,
506 1964.
507 Dansgaard, W. and Johnsen, S.: A flow model and a time scale for the ice core from Camp Century, Greenland, J. Glaciol.,
508 8, 215– 223, 1969.
509 DeConto, R. M. and Pollard, D.: Contribution of Antarctica to past and future sea-level rise, Nature, 531(7596),
510 https://doi.org/10.1038/nature17145, 2016.
511 de Leeuw, G., Andreas, E. L., Anguelova, M. D., Fairall, C. W., Lewis, E. R., O'Dowd, C., Schulz, M., Schwartz, S. E.:
512 Production flux of sea salt aerosol, Reviews of Geophysics, 49, Rg2001, 2011
513 Delmas, R. J., Legrand, M., Aristarain, A. J. and Zanolini, F.: Volcanic deposits in Antarctic snow and ice., Journal of
514 Geophysical Research, 90(D7), 12901–12920, https://doi.org/10.1029/JD090iD07p12901, 1985.
515 Delmonte, B., Petit, J. and Maggi, V.: Glacial to Holocene implications of the new 27000-year dust record from the EPICA
516 Dome C (East Antarctica) ice core, Climate Dynamics, 18(8), 647–660, https://doi.org/10.1007/s00382-001-0193-9, 2002.
517 Dibb, J. E., Talbot, R. W., Munger, J. W., Jacob, D. J. and Fan, S. M.: Air-snow exchange of HNO3 and NOy at Summit,
518 Greenland, Journal of Geophysical Research Atmospheres, 103(D3), 3475–3486, https://doi.org/10.1029/97JD03132, 1998.

519 Epstein, S. and Mayeda, T.: Variation of O18 content of waters from natural sources, Geochimica et Cosmochimica Acta,
520 4(5), https://doi.org/10.1016/0016-7037(53)90051-9, 1953.
521 Erbland, J., Vicars, W. C., Savarino, J., Morin, S., Frey, M. M., Frosini, D., Vince, E. and Martins, J. M. F.: Air-snow
522 transfer of nitrate on the East Antarctic Plateau - Part 1: Isotopic evidence for a photolytically driven dynamic equilibrium in
523 summer, Atmospheric Chemistry and Physics, 13(13), 6403–6419, https://doi.org/10.5194/acp-13-6403-2013, 2013.
524 Extier, T., Landais, A., Bréant, C., Prié, F., Bazin, L., Dreyfus, G., Roche, D. M. and Leuenberger, M.: On the use of
525 δ18Oatm for ice core dating, Quaternary Science Reviews, 185, 244–257, https://doi.org/10.1016/j.quascirev.2018.02.008,
526 2018.
527 Fischer, H., Fundel, F., Ruth, U., Twarloh, B., Wegner, A., Udisti, R., Becagli, S., Castellano, E., Morganti, A., Severi, M.,
528 Wolff, E., Littot, G., Röthlisberger, R., Mulvaney, R., Hutterli, M. A., Kaufmann, P., Federer, U., Lambert, F., Bigler, M.,
529 Hansson, M., Jonsell, U., de Angelis, M., Boutron, C., Siggaard-Andersen, M. L., Steffensen, J. P., Barbante, C., Gaspari,
530 V., Gabrielli, P. and Wagenbach, D.: Reconstruction of millennial changes in dust emission, transport and regional sea ice
531 coverage using the deep EPICA ice cores from the Atlantic and Indian Ocean sector of Antarctica, Earth and Planetary
532 Science Letters, 260(1–2), 340–354, https://doi.org/10.1016/j.epsl.2007.06.014, 2007.
533 Fretwell, P., Pritchard, H. D., Vaughan, D. G., Bamber, J. L., Barrand, N. E., Bell, R., Bianchi, C., Bingham, R. G.,
534 Blankenship, D. D., Casassa, G., Catania, G., Callens, D., Conway, H., Cook, A. J., Corr, H. F. J., Damaske, D., Damm, V.,
535 Ferraccioli, F., Forsberg, R., Fujita, S., Gim, Y., Gogineni, P., Griggs, J. A., Hindmarsh, R. C. A., Holmlund, P., Holt, J. W.,
536 Jacobel, R. W., Jenkins, A., Hokat, W., Jordan, T., King, E. C., Kohler, J., Krabill, W., Riger-Kusk, M., Langley, K.A.,
537 Leitchenkov, G., Leuschen, C., Luyendyk, B. P., Matsuoka, K., Mouginot, J., Nitsche, F. O., Nogi, N., Nost, O. A., Popov,
538 S. V., Rignot, E., Rippin, D. M., Rivera, A., Roberts, J., Ross, N., Siegert, M. J., Smith, A. M., Steinhage, D., Studinger, M.,
539 Sun, B., Tinto, K., Welch, B. C., Wilson, D., Young, D. A., Xiangbin, C., Zirizzotti, A.: Bedmap2: Improved Ice Bed,
540 Surface and Thickness Dataset for Antarctica, The Cryosphere, 7(1), 375-393, 2013.
541 Frezzotti, M., Urbini, S., Proposito, M., Scarchilli, C. and Gandolfi, S.: Spatial and temporal variability of surface mass
542 balance near Talos Dome, East Antarctica, Journal of Geophysical Research: Earth Surface, 112(2),
543 https://doi.org/10.1029/2006JF000638, 2007.
544 Frezzotti, M., Scarchilli, C., Becagli, S., Proposito, M. and Urbini, S.: A synthesis of the Antarctic surface mass balance
545 during the last 800 yr, The Cryosphere, 7(1), https://doi.org/10.5194/tc-7-303-2013, 2013.
546 Gondwe, M., Krol, M., Gieskes, W., Klaassen, W. and de Baar, H.: The contribution of ocean-leaving DMS to the global
547 atmospheric burdens of DMS, MSA, SO 2 , and NSS SO 4 = , Global Biogeochemical Cycles, 17(2), n/a-n/a,
548 https://doi.org/10.1029/2002gb001937, 2003.
549 Grannas, A. M., Jones, A. E., Dibb, J., Ammann, M., Anastasio, C., Beine, H. J., Bergin, M., Bottenheim, J., Boxe, C. S.,
550 Carver, G., Chen, G., Crawford, J. H., Dominé, F., Frey, M. M., Guzmán, M. I., Heard, D. E., Helmig, D., Hoffmann, M. R.,
551 Honrath, R. E., Huey, L. G., Hutterli, M., Jacobi, H. W., Klán, P., Lefer, B., Mcconnell, J., Plane, J., Sander, R., Savarino, J.,

552 Shepson, P. B., Simpson, W. R., Sodeau, J. R., von Glasow, R., Weller, R., Wolff, E. W. and Zhu, T.: An overview of snow
553 photochemistry: evidence, mechanisms and impacts, Atmospheric Chemistry and Physics, 7(16), 4329-4373, 2007.
554 Greene, C. A., Gwyther, D. E., Blankenship, D. D.: Antarctic Mapping Tools for Matlab, Computers & Geosciences, 104,
555 151-157, 2017.
556 Hammer, C. U.: Acidity of Polar Ice Cores in Relation to Absolute Dating, Past Volcanism, and Radio–Echoes, Journal of
557 Glaciology, 25(93), 359–372, 1980.
558 Hastings, M. G., Sigman, D. M. and Steig, E. J.: Glacial/interglacial changes in the isotopes of nitrate from the Greenland Ice
559 Sheet Project 2 (GISP2) ice core, Global Biogeochemical Cycles, 19(4), https://doi.org/10.1029/2005GB002502, 2005.
560 Herron, M. M. and Langway, C. C.: Dating of Ross Ice Shelf Core by chemical analysis, Journal of Glaciology, 24(90),
561 1979.
562 Hwang, H., Hur, S. do, Lee, J., Han, Y., Hong, S. and Motoyama, H.: Plutonium fallout reconstructed from an Antarctic
563 Plateau snowpack using inductively coupled plasma sector field mass spectrometry, Science of the Total Environment, 669,
564 505–511, https://doi.org/10.1016/j.scitotenv.2019.03.105, 2019.
565 Igarashi, M., Nakai, Y., Motizuki, Y., Takahashi, K., Motoyama, H. and Makishima, K.: Dating of the Dome Fuji shallow
566 ice core based on a record of volcanic eruptions from AD 1260 to AD 2001, Polar Science, 5(4), 411–420,
567 https://doi.org/10.1016/j.polar.2011.08.001, 2011.
568 Jones, J. M., Gille, S. T., Goosse, H., Abram, N. J., Canziani, P. O., Charman, D. J., Clem, K. R., Crosta, X., de Lavergne,
569 C., Eisenman, I., England, M. H., Fogt, R. L., Frankcombe, L. M., Marshall, G. J., Masson-Delmotte, V., Morrison, A. K.,
570 Orsi, A. J., Raphael, M. N., Renwick, J. A., Schneider, D. P., Simpkins, G. R., Steig, E. J., Stenni, B., Swingedouw, D. and
571 Vance, T. R.: Assessing recent trends in high-latitude Southern Hemisphere surface climate, Nature Climate Change, 6(10),
572 917–926, https://doi.org/10.1038/nclimate3103, 2016.
573 Kellerhals, T., Tobler, L., Brütsch, S., Sigl, M., Wacker, L., Gäggeler, H. W. and Schwikowski, M.: Thallium as a Tracer for
574 Preindustrial Volcanic Eruptions in an Ice Core Record from Illimani, Bolivia, Environmental Science & Technology, 44(3),
575 https://doi.org/10.1021/es902492n, 2010.
576 Krinner, G., Magand, O., Simmonds, I., Genthon, C. and Dufresne, J. L.: Simulated Antarctic precipitation and surface mass
577 balance at the end of the twentieth and twenty-first centuries, Climate Dynamics, 28(2–3), 215–230,
578 https://doi.org/10.1007/s00382-006-0177-x, 2007.
579 Legrand, M., Wolff, E. and Wagenbach, D.: Antarctic aerosol and snowfall chemistry: implications for deep Antarctic ice-
580 core chemistry, Annals of Glaciology, 29, 66-72, 1999.
581 Legrand, M. R. and Delmas, R. J.: The ionic balance of Antarctic snow: A 10-year detailed record, Atmospheric
582 Environment, 18(9), 1867–1874, 1984.
583 Magand, O., Frezzotti, M., Pourchet, M., Stenni, B., Genoni, L. and Fily, M.: Climate variability along latitudinal and
584 longitudinal transects in East Antarctica., Annals of Glaciology, 39, 351-358, 2004.

585 Maupetit, F. and Delmas, R. J.: Chemical composition of Falling Snow at Dumont D'Urville, Antarctica, Journal of
586 Atmospheric Chemistry, 14, 31–42, 1992.
587 Morganti, A., Becagli, S., Castellano, E., Severi, M., Traversi, R. and Udisti, R.: An improved flow analysis-ion
588 chromatography method for determination of cationic and anionic species at trace levels in Antarctic ice cores, Analytica
589 Chimica Acta, 603(2), 190–198, https://doi.org/10.1016/j.aca.2007.09.050, 2007.
590 Mulvaney, R., Wagenbach, D., Wolff, E. W.: Postdepositional change in snowpack nitrate from observation of year-round
591 near-surface snow in coastal Antarctica, Journal of Geophysical Research: Atmospheres, 103(D9), 11021-11031, 1998.
592 Mulvaney, R. and Wolff, E. W.: Spatial variability of the major chemistry of the Antarctic ice sheet, Annals of Glaciology,
593 20, 440–447, https://doi.org/10.3189/1994aog20-1-440-447, 1994.
594 Narcisi, B. and Petit, J. R.: Englacial tephras of East Antarctica, edited by J. Smellie, K. Panter, and A. Geyer, Geological
595 Society, London, 2021.
596 Narcisi, B., Proposito, M. and Frezzotti, M.: Ice record of a 13th century explosive volcanic eruption in northern Victoria
597 Land, East Antarctica, Antarctic Science, 13(2), 174–181, https://doi.org/10.1017/S0954102001000268, 2001.
598 Narcisi, B., Petit, J. R., Delmonte, B., Scarchilli, C. and Stenni, B.: A 16,000-yr tephra framework for the Antarctic ice sheet:
599 A contribution from the new Talos Dome core, Quaternary Science Reviews, 49, 52–63,
600 https://doi.org/10.1016/j.quascirev.2012.06.011, 2012.
601 Nardin, R., Amore, A., Becagli, S., Caiazzo, L., Frezzotti, M., Severi, M., Stenni, B. and Traversi, R.: Volcanic Fluxes Over
602 the Last Millennium as Recorded in the GV7 Ice Core (Northern Victoria Land, Antarctica), Geosciences, 10(1), 38,
603 https://doi.org/10.3390/geosciences10010038, 2020.
604 Neukom, R., Schurer, A. P., Steiger, Nathan. J. and Hegerl, G. C.: Possible causes of data model discrepancy in the
605 temperature history of the last Millennium, Scientific Reports, 8(1), 7572, https://doi.org/10.1038/s41598-018-25862-2,
606 2018.
607 Nozaki, Y.: A fresh look at element distribution in the North Pacific Ocean, Eos, 78(21), 221,
608 https://doi.org/10.1029/97eo00148, 1997.
609 Nyamgerel, Y., Han, Y., Kim, S., Hong, S.-B., Lee, J. and Hur, S. do: Chronological characteristics for snow accumulation
610 on Styx Glacier in northern Victoria Land, Antarctica, Journal of Glaciology, 1–11, https://doi.org/10.1017/jog.2020.53,
611 2020.
612 Pasteris, D. R., McConnell, J. R., Das, S. B., Criscitiello, A. S., Evans, M. J., Maselli, O. J., Sigl, M. and Layman, L.:
613 Seasonally resolved ice core records from West Antarctica indicate a sea ice source of sea-salt aerosol and a biomass burning
614 source of ammonium, Journal of Geophysical Research, 119(14), 9168–9182, https://doi.org/10.1002/2013JD020720, 2014.
615 Piccardi, G., Udisti, R. and Casella, F.: Seasonal trends and chemical composition of snow at terra nova bay (antarctica),
616 International Journal of Environmental Analytical Chemistry, 55(1–4), 219–234,
617 https://doi.org/10.1080/03067319408026220, 1994.

Rasmussen, S. O., Andersen, K. K., Svensson, A. M., Steffensen, J. P., Vinther, B. M., Clausen, H. B., Siggaard-Andersen, M. L., Johnsen, S. J., Larsen, L. B., Dahl-Jensen, D., Bigler, M., Röthlisberger, R., Fischer, H., Goto-Azuma, K., Hansson, M. E. and Ruth, U.: A new Greenland ice core chronology for the last glacial termination, Journal of Geophysical Research Atmospheres, 111(6), https://doi.org/10.1029/2005JD006079, 2006.

Roberts, J., Plummer, C., Vance, T., van Ommen, T., Moy, A., Poynter, S., Treverrow, A., Curran, M. and George, S.: A 2000-year annual record of snow accumulation rates for Law Dome, East Antarctica, Climate of the Past, 11(5), 697-707, 2015.

Röthlisberger, R., Hutterli, M. A., Sommer, S., Wolff, E. W. and Mulvaney, R.: Factors controlling nitrate in ice cores: Evidence from the Dome C deep ice core, Journal of Geophysical Research Atmospheres, 105(D16), 20565–20572, https://doi.org/10.1029/2000JD900264, 2000.

Röthlisberger, R., Hutterli, M. A., Wolff, E. W., Mulvaney, R., Fischer, H., Bigler, M., Goto-Azuma, K., Hansson, M. E., Ruth, U., Siggaard-Andersen, M.-L. and Steffensen, J. P.: Nitrate in Greenland and Antarctic ice cores: a detailed description of post-depositional processes, Annals of Glaciology, 35, 209-216, 2002.

Scarchilli, C., Frezzotti, M. and Ruti, P. M.: Snow precipitation at four ice core sites in East Antarctica: provenance, seasonality and blocking factors, Climate Dynamics, 37(9–10), 2107–2125, https://doi.org/10.1007/s00382-010-0946-4, 2011.

Severi, M., Becagli, S., Castellano, E., Morganti, A., Traversi, R., Udisti, R., Ruth, U., Fischer, H., Huybrechts, P., Wolff, E., Parrenin, F., Kaufmann, P., Lambert, F. and Steffensen, J. P.: Synchronisation of the EDML and EDC ice cores for the last 52 kyr by volcanic signature matching, Climate of the Past, 3(3), 367–374, https://doi.org/10.5194/cp-3-367-2007, 2007.

Severi, M., Udisti, R., Becagli, S., Stenni, B. and Traversi, R.: Volcanic synchronisation of the EPICA-DC and TALDICE ice cores for the last 42 kyr BP, Climate of the Past, 8(2), 509–517, https://doi.org/10.5194/cp-8-509-2012, 2012.

Shi, G., Chai, J., Zhu, Z., Hu, Z., Chen, Z., Yu, J., Ma, T., Ma, H., An, C., Jiang, S., Tang, X., Hastings, M. G.: Isotope Fractionation of Nitrate During Volatilization in Snow: A Field Investigation in Antarctica, Geophysical Research Letters, 46(6), 3287-3297, https://doi.org/10.1029/2019GL081968, 2015.

Sigl, M., McConnell, J. R., Layman, L., Maselli, O., McGwire, K., Pasteris, D., Dahl-Jensen, D., Steffensen, J. P., Vinther, B., Edwards, R., Mulvaney, R. and Kipfstuhl, S.: A new bipolar ice core record of volcanism from WAIS Divide and NEEM and implications for climate forcing of the last 2000 years, Journal of Geophysical Research Atmospheres, 118(3), 1151–1169, https://doi.org/10.1029/2012JD018603, 2013.

Sigl, M., Winstrup, M., McConnell, J. R., Welten, K. C., Plunkett, G., Ludlow, F., Büntgen, U., Caffee, M., Chellman, N., Dahl-Jensen, D., Fischer, H., Kipfstuhl, S., Kostick, C., Maselli, O. J., Mekhaldi, F., Mulvaney, R., Muscheler, R., Pasteris, D. R., Pilcher, J. R., Salzer, M., Schüpbach, S., Steffensen, J. P., Vinther, B. M. and Woodruff, T. E.: Timing and climate forcing of volcanic eruptions for the past 2,500 years, Nature, 523(7562), 543–549, https://doi.org/10.1038/nature14565, 2015.

Sigl, M., Fudge, T. J., Winstrup, M., Cole-Dai, J., Ferris, D., McConnell, J. R., Taylor, K. C., Welten, K. C., Woodruff, T. E., Adolphi, F., Bisiaux, M., Brook, E. J., Buizert, C., Caffee, M. W., Dunbar, N. W., Edwards, R., Geng, L., Iverson, N., Koffman, B., Layman, L., Maselli, O. J., McGwire, K., Muscheler, R., Nishiizumi, K., Pasteris, D. R., Rhodes, R. H. and Sowers, T. A.: The WAIS Divide deep ice core WD2014 chronology - Part 2: Annual-layer counting (0-31 ka BP), Climate of the Past, 12(3), 769–786, https://doi.org/10.5194/cp-12-769-2016, 2016.

Sodemann, H. and Stohl, A.: Asymmetries in the moisture origin of Antarctic precipitation, Geophysical Research Letters, 36(22), https://doi.org/10.1029/2009GL040242, 2009.

Stefels, J., Steinke, M., Turner, S., Malin, G. and Belviso, S.: Environmental constraints on the production and removal of the climatically active gas dimethylsulphide (DMS) and implications for ecosystem modelling, in Biogeochemistry, 83, 245–275, https://doi.org/10.1007/s10533-007-9091-5, 2007.

Stenni, B., Masson-Delmotte, V., Johnsen, S. J., Jouzel, J., Longinelli, A., Monnin, E., Rothlisberger, R., Selmo, E.: An Oceanic Cold Reversal During the Last Deglaciation, Science, 293(5537), 2074-2077, 2001

Stenni, B., Proposito, M., Gragnani, R., Flora, O., Jouzel, J., Falourd, S. and Frezzotti, M.: Eight centuries of volcanic signal and climate change at Talos Dome (East Antarctica), Journal of Geophysical Research D: Atmospheres, 107(9–10), 3–1, https://doi.org/10.1029/2000jd000317, 2002.

Tao, G., Yamada, R., Fujikawa, Y., Kudo, A., Zheng, J., Fisher, D. A. and Koerner, R. M.: Determination of trace amounts of heavy metals in arctic ice core samples using inductively coupled plasma mass spectrometry. Talanata, 55(4):765-72, doi: 10.1016/s0039-9140(01)00509-4, 2001.

Thomas, E. R., Wolff, E. W., Mulvaney, R., Steffensen, J. P., Johnsen, S. J., Arrowsmith, C., White, J. W. C., Vaughn, B. and Popp, T.: The 8.2 ka event from Greenland ice cores, Quaternary Science Reviews, 26(1–2), 70–81, https://doi.org/10.1016/j.quascirev.2006.07.017, 2007.

Thomas, E. R., Melchior Van Wessem, J., Roberts, J., Isaksson, E., Schlosser, E., Fudge, T. J., Vallelonga, P., Medley, B., Lenaerts, J., Bertler, N., van den Broeke, M. R., Dixon, D. A., Frezzotti, M., Stenni, B., Curran, M. and Ekaykin, A. A.: Regional Antarctic snow accumulation over the past 1000 years, Climate of the Past, 13(11), 1491–1513, https://doi.org/10.5194/cp-13-1491-2017, 2017.

Tomé, A., and Miranda, P. M. A.: Piecewise linear fitting and trend changing points of climate parameters, Geophysical Research Letters, 31(2), L02207, doi:10.1029/2003GL019100, 2004

Traufetter, F., Oerter, H., Fischer, H., Weller, R. and Miller, H.: Spatio-temporal variability in volcanic sulphate deposition over the past 2 kyr in snow pits and firn cores from Amundsenisen, Antarctica, Journal of Glaciology,50(168), 137-146, 2004.

Traversi, R., Usoskin, I. G., Solanki, S. K., Becagli, S., Frezzotti, M., Severi, M., Stenni, B. and Udisti, R.: Nitrate in Polar Ice: A New Tracer of Solar Variability, Solar Physics, 280(1), 237–254, https://doi.org/10.1007/s11207-012-0060-3, 2012.

Udisti, R.: Multiparametric approach for chemical dating of snow layers from Antarctica, International Journal of Environmental Analytical Chemistry, 63(3), 225–244, https://doi.org/10.1080/03067319608026268, 1996.

685 Udisti, R., Dayan, U., Becagli, S., Busetto, M., Frosini, D., Legrand, M., Lucarelli, F., Preunkert, S., Severi, M., Traversi, R.
686 and Vitale, V.: Sea spray aerosol in central Antarctica. Present atmospheric behaviour and implications for paleoclimatic
687 reconstructions, Atmospheric Environment, 52, 109–120, https://doi.org/10.1016/j.atmosenv.2011.10.018, 2012.
688 Van Ommen, T., Morgan, V., Curran, M., Declacial and Holocene changes in accumulation at Law Dome, East Antarctica,
689 Annals of Glaciology, 39, 359-365, 2004.
690 Van omen, T. and Morgan, V., Snowfall increase in coastal East Antarctica linked with southwest Western Australian
691 drought, Nature Geoscience, 3(4), 267-272, 2010.
692 Vance, T. R., Roberts, J. L., Plummer, C. T., Kiem, A. S., van Ommen, T. D.; Inderdecadal Pacific variability and eastern
693 Australian megadroughts over the last millennium, Geophysical Research Letters, 42(1), 129-137, 2015.
694 Watanabe, O., Kamiyama, K., Motoyama, H., Fujii, Y., Shoji, H. and Satow, K.: The paleoclimate record in the ice core at
695 Dome Fuji station, East Antarctica., 1999.
696 Weller, R., Wagenbach, D., Legrand, M., Elsässer, C., Tian-Kunze, X. and König-Langlo, G.: Continuous 25-yr aerosol
697 records at coastal Antarctica - I: Inter-annual variability of ionic compounds links to climate indices, Tellus, Series B:
698 Chemical and Physical Meteorology, 63(5), 901–919, https://doi.org/10.1111/j.1600-0889.2011.00542.x, 2011.
699 Winski, D. A., Fudge, T. J., Ferris, D. G., Osterberg, E. C., Fegyveresi, J. M., Cole-Dai, J., Thundercloud, Z., Cox, T. S.,
700 Kreutz, K. J., Ortman, N., Buizert, C., Epifanio, J., Brook, E. J., Beaudette, R., Severinghaus, J., Sowers, T., Steig, E. J.,
701 Kahle, E. C., Jones, T. R., Morris, V., Aydin, M., Nicewonger, M. R., Casey, K. A., Alley, R. B., Waddington, E. D.,
702 Iverson, N. A., Dunbar, N. W., Bay, R. C., Souney, J. M., Sigl, M. and McConnell, J. R.: The SP19 chronology for the South
703 Pole Ice Core - Part 1: Volcanic matching and annual layer counting, Climate of the Past, 15(5), 1793–1808,
704 https://doi.org/10.5194/cp-15-1793-2019, 2019.
705 Winstrup, M., Svensson, A. M., Rasmussen, S. O., Winther, O., Steig, E. J., Axelrod, A. E.: An automated approach for
706 annual layer counting in ice cores, Climate of the past 8, 1881-1895, 2012
707 Winstrup, M., Vallelonga, P., Kjaer, H. A., Fudge, T. K., Lee. J. E., Riis, M. H.; Edwards, R., Bertler, N. A. N., Blunier, T.,
708 Brook, E. J., Buizert, N. A. N., Ciobanu, G., Conway, H., Dahl-Jensen, D., Ellis, A., Emanuelsson, B. D., Hindmarsch, R. C.
709 A., Keller, E. D., Kurbatov, A. V., Mayewski, P. A., Neff, P. D., Pyne, R. L., Simonsen, M. F., Svensson, A., Tuohy, A.,
710 Waddington, E. D., Wheatley, S.: A 2700-year annual timescale and accumulation history for an ice from Roosevelt Island,
711 West Antarctica, Climate of the Past, 15, 751-779, 2019
712 Wolff, E. W.: Nitrate in Polar Ice, in Ice Core Studies of Global Biogeochemical Cycles, Springer Berlin Heidelberg, Berlin,
713 Heidelberg, https://doi.org/10.1007/978-3-642-51172-1_10, , 1995.
714 Wolff, E. W.: Ice sheets and nitrogen., Philosophical transactions of the Royal Society of London. Series B, Biological
715 sciences, 368(1621), 20130127, https://doi.org/10.1098/rstb.2013.0127, 2013.
716 Wolff, E. W., Barbante, C., Becagli, S., Bigler, M., Boutron, C. F., Castellano, E., de Angelis, M., Federer, U., Fischer, H.,
717 Fundel, F., Hansson, M., Hutterli, M., Jonsell, U., Karlin, T., Kaufmann, P., Lambert, F., Littot, G. C., Mulvaney, R.,
718 Röthlisberger, R., Ruth, U., Severi, M., Siggaard-Andersen, M. L., Sime, L. C., Steffensen, J. P., Stocker, T. F., Traversi, R.,

Twarloh, B., Udisti, R., Wagenbach, D. and Wegner, A.: Changes in environment over the last 800,000 years from chemical analysis of the EPICA Dome C ice core, Quaternary Science Reviews, 29(1–2), 285–295, https://doi.org/10.1016/j.quascirev.2009.06.013, 2010.

Zatko, M., Geng, L., Alexander, B., Sofen, E., and Klein, K.: The impact of snow nitrate photolysis on boundary layer chemistry and the recycling and redistribution of reactive nitrogen across Antarctica and Greenland in a global chemical transport model, Atmos. Chem. Phys., 16, 2819–2842, https://doi.org/10.5194/acp-16-2819-2016, 2016.

Zielinski, G. A., Mayewski, P. A., David Meeker, L., Whitlow, S. and Twickler, M. S.: A 110,000-Yr Record of Explosive Volcanism from the GISP2 (Greenland) Ice Core, Quaternary Research 45(2), 109-118, 1996.